



HAL
open science

Stochastic Analysis of Empty-Region Graphs

Olivier Devillers, Charles Duménil

► **To cite this version:**

Olivier Devillers, Charles Duménil. Stochastic Analysis of Empty-Region Graphs. CCCG 2021 - 33rd Canadian Conference on Computational Geometry, Aug 2021, Halifax / Virtual, Canada. hal-03296186

HAL Id: hal-03296186

<https://hal.inria.fr/hal-03296186>

Submitted on 22 Jul 2021

HAL is a multi-disciplinary open access archive for the deposit and dissemination of scientific research documents, whether they are published or not. The documents may come from teaching and research institutions in France or abroad, or from public or private research centers.

L'archive ouverte pluridisciplinaire **HAL**, est destinée au dépôt et à la diffusion de documents scientifiques de niveau recherche, publiés ou non, émanant des établissements d'enseignement et de recherche français ou étrangers, des laboratoires publics ou privés.

Stochastic Analysis of Empty-Region Graphs

Olivier Devillers*

Charles Duménil*

Abstract

Given a set of points X , an empty-region graph is a graph in which $p, q \in X$ are neighbors if some region defined by (p, q) does not contain any point of X . We provide expected analyses of the degree of a point and the possibility of having *far* neighbors in such a graph when X is a planar Poisson point process. Namely the expected degree of a point in the empty axis-aligned-ellipse graph for a Poisson point process of intensity λ in the unit square is $\Theta(\ln \lambda)$. It is $\Theta(\ln \beta)$ if the ellipses are constrained to have an aspect ratio between 1 and $\beta > 1$, and $\Theta(\beta)$ when the aspect ratio is constrained but ellipses are not axis-aligned.

1 Introduction

We start by defining the notion of empty-region graph [2]:

Definition 1 For each pair $(p, q) \in \mathbb{R}^d \times \mathbb{R}^d$, let $\mathcal{R}(p, q)$ be a family of regions. Consider a locally finite point set $X \subset \mathbb{R}^d$. We denote by $\mathcal{G}_{\mathcal{R}}^{\emptyset}(X)$ the graph on X in which p is a neighbor of q if and only if there exists an empty region in $\mathcal{R}(p, q)$.

This notion unifies the classical Delaunay triangulation [3] where $\mathcal{R}(p, q)$ is the set of disks whose boundaries contains p and q , the Gabriel graph [6] where $\mathcal{R}(p, q)$ is reduced to the disk of diameter pq , the β -skeleton [7, 1], the empty-ellipse graph [4], the nearest neighbor-graph, the Θ -graphs, and the Yao graphs [9].

In this paper, we will assume that X is a Poisson point process in the plane and compute quantities like the expected degree of a point $p \in X$ in $\mathcal{G}_{\mathcal{R}}^{\emptyset}(X)$ or the probability that p has neighbors further than some threshold. Computing such quantities when $\mathcal{R}(p, q)$ is a singleton, as for the Gabriel graph, is much easier than when it is a bigger set, as for Delaunay triangulation. To this aim, it is interesting to try to get upper and lower bounds by comparing empty-region graphs. This idea was already used by Devroye, Lemaire and Moreau [5] to bounds the size of the Delaunay triangulation by the sizes of the Gabriel graph and the half-moon graph.

In this paper we formalize the process through two lemmas: the Combination lemma and the Partition lemma, and we illustrate these tools with empty-ellipse graphs. In a forthcoming paper we apply these results to equations of higher degree appearing when parameterizing 3D surfaces.

2 First Example: Delaunay and Gabriel Graphs

2.1 Delaunay Triangulation

The Delaunay triangulation is the empty-region graph where $\mathcal{R}(p, q) = \{D(p, q, r); r \in \mathbb{R}^2\}$ and $D(p, q, r)$ is the open disk with p, q , and r on its boundary.

Although the expected degree of a random point in any kind of triangulation is well known to be 6 using Euler formula, we prove it using stochastic tools to illustrate the complexity of such a computation:

Theorem 2 Let X be a Poisson point process with intensity λ in \mathbb{R}^2 and p a point of \mathbb{R}^2 . The expected degree $\mathbb{E}[\deg(p, \text{Del})]$ of p in the Delaunay triangulation $\text{Del}(X \cup \{p\})$ is 6.

Proof. Without loss of generality, we assume that p is at the origin. Let $D(p, q, r)$ denote the open disk with p, q , and r on its boundary. The number of neighbors of p in $\text{Del}(X \cup \{p\})$ is the number of distinct sets $\{q, r\}$ in X^2 with $q \neq r$ such that $D(p, q, r)$ does not contain any point of X . It is given by the random value: $\deg(p, \text{Del}) = \frac{1}{2} \sum_{q \in X} \sum_{r \in X \setminus \{q\}} \mathbb{1}_{[D(p, q, r) \cap X = \emptyset]}$, where the factor $\frac{1}{2}$ corrected the double counting of each set $\{q, r\}$ in the sum. We compute the expectation of this formula:

$$\begin{aligned} \mathbb{E}[\deg(p, \text{Del})] &= \mathbb{E} \left[\frac{1}{2} \sum_{q \in X} \sum_{r \in X \setminus \{q\}} \mathbb{1}_{[D(p, q, r) \cap X = \emptyset]} \right] \\ &= \frac{1}{2} \int_{\mathbb{R}^2} \int_{\mathbb{R}^2} \lambda^2 \mathbb{P}[D(p, q, r) \cap X = \emptyset] \, dr dq \\ &\quad \text{by Slivnyak-Mecke Theorem [8]} \\ &= \frac{1}{2} \int_{\mathbb{R}^2} \int_{\mathbb{R}^2} \lambda^2 e^{-\lambda |D(p, q, r)|} \, dr dq \\ &\quad \text{by definition of Poisson point process.} \end{aligned}$$

The computation of this integral is a bit technical and is given in appendix. It involves a Blaschke-Petkantschin like variables substitution to turn the

*Université de Lorraine, CNRS, Inria, LORIA, F-54000 Nancy, France. `FirstName.LastName@inria.fr`. This research has been funded by grant ANR-17-CE40-0017 of the French National Research Agency (Aspag)

cartesian coordinates of q and r in the coordinate of the center of $D(p, q, r)$ and two angles to place q and r on the boundary of $D(p, q, r)$.

It finally turns out that the value of this integral is 6, as anticipated. \square

2.2 Gabriel Graph and Half-Moon Graph

We now turn our interest to cases where $\mathcal{R}(p, q)$ is a singleton. We consider the three following possibilities: $\mathcal{R}(p, q) = \{\text{Gab}(p, q)\}$ the disk of diameter pq , $\mathcal{R}(p, q) = \{hm_r(p, q)\}$ the half-disk of diameter pq to the right of pq , and $\mathcal{R}(p, q) = \{hm_\ell(p, q)\}$ the half-disk of diameter pq to the left of pq . Then $\mathcal{G}_{\{\text{Gab}\}}^\emptyset$ is the Gabriel graph, $\mathcal{G}_{\{hm_r\}}^\emptyset$ is the right half-moon graph, and $\mathcal{G}_{\{hm_\ell\}}^\emptyset$ is the left half-moon graph. The half-moon graph is $\mathcal{G}_{\{hm_r\}}^\emptyset \cup \mathcal{G}_{\{hm_\ell\}}^\emptyset$.

Lemma 3 *Let X be a Poisson point process with intensity λ in \mathbb{R}^2 and p a point of \mathbb{R}^2 . The expected degree $\mathbb{E} \left[\deg \left(p, \mathcal{G}_{\{\text{Gab}\}}^\emptyset \right) \right]$ of the origin p in the Gabriel graph $\mathcal{G}_{\{\text{Gab}\}}^\emptyset(X)$ is 4.*

Proof.

$$\begin{aligned} \mathbb{E} \left[\deg \left(p, \mathcal{G}_{\{\text{Gab}\}}^\emptyset \right) \right] &= \mathbb{E} \left[\sum_{q \in X} \mathbb{1}_{[\text{Gab}(p, q) \cap X = \emptyset]} \right] \\ &= \int_{q \in \mathbb{R}^2} \lambda \mathbb{P}[\text{Gab}(p, q) \cap X = \emptyset] dq \\ &= \int_{\mathbb{R}^2} \lambda e^{-\lambda |\text{Gab}(p, q)|} dq \\ &= \int_{\mathbb{R}^+} \int_0^{2\pi} \lambda e^{-\lambda \frac{\pi \rho^2}{4}} \rho d\theta d\rho = 4. \quad \square \end{aligned}$$

Lemma 4 *Let X be a Poisson point process with intensity λ in \mathbb{R}^2 and p a point of \mathbb{R}^2 . Then*

$$\mathbb{E} \left[\deg \left(p, \mathcal{G}_{\{hm_r\}}^\emptyset \right) \right] = \mathbb{E} \left[\deg \left(p, \mathcal{G}_{\{hm_\ell\}}^\emptyset \right) \right] = 8.$$

Proof. By symmetry, we only do the computation for $\mathbb{E} \left[\deg \left(p, \mathcal{G}_{\{hm_r\}}^\emptyset \right) \right]$.

$$\begin{aligned} \mathbb{E} \left[\deg \left(p, \mathcal{G}_{\{hm_r\}}^\emptyset \right) \right] &= \mathbb{E} \left[\sum_{q \in X} \mathbb{1}_{[hm_r(p, q) \cap X = \emptyset]} \right] \\ &= \int_{\mathbb{R}^2} \lambda e^{-\lambda |hm_r(p, q)|} dq \\ &= \int_{\mathbb{R}^+} \int_0^{2\pi} \lambda e^{-\lambda \frac{\pi \rho^2}{8}} \rho d\theta d\rho = 8. \quad \square \end{aligned}$$

As one can see, the fact that $\mathcal{R}(p, q)$ is a singleton made the computation much simpler than in the case of the Delaunay triangulation.

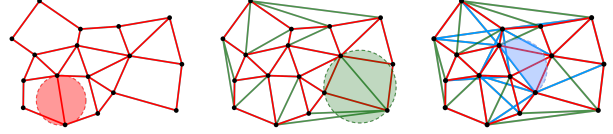


Figure 1: The Gabriel graph, on the left, is included in the Delaunay triangulation, in the middle, itself included in the half-moon graph, on the right.

2.3 Graph Relations

The following relations between the graphs are straightforward since any disk with p and q on its boundary contains either $hm_r(p, q)$ or $hm_\ell(p, q)$ (see Figure 1):

$$\begin{aligned} \mathcal{G}_{\{\text{Gab}\}}^\emptyset &= \mathcal{G}_{\{hm_r\}}^\emptyset \cap \mathcal{G}_{\{hm_\ell\}}^\emptyset, \\ \mathcal{G}_{\{\text{Gab}\}}^\emptyset \subset \text{Del} &\subset \mathcal{G}_{\{hm_r\}}^\emptyset \cup \mathcal{G}_{\{hm_\ell\}}^\emptyset = \mathcal{G}_{\{hm_r, hm_\ell\}}^\emptyset. \end{aligned}$$

From this, we deduce

$$\begin{aligned} \deg \left(p, \mathcal{G}_{\{\text{Gab}\}}^\emptyset \right) &\leq \deg \left(p, \text{Del} \right) \leq \deg \left(p, \mathcal{G}_{\{hm_r, hm_\ell\}}^\emptyset \right) \\ 4 &\leq \deg \left(p, \text{Del} \right) \leq 8 + 8 - 4 = 12. \end{aligned}$$

This result is weaker than the exact bound of Theorem 2 but the computations are much simpler. It also illustrates that, given regions of similar areas, the degree remains of equal order of magnitude. In that case, for two points p and q , $\text{Gab}(p, q)$ and $hm_r(p, q)$ or $hm_\ell(p, q)$ have both an area quadratic in the distance between p and q , and this induces a constant expected degree.

3 General Method

We propose a general method that both formalizes and generalizes the half-moon method to link the degree in empty-region graphs to the degree in empty-region graphs defined by singletons. We formalize the following facts: (i) the Delaunay disks can be parameterized by their center on the bisector of pq , (ii) this bisector can be partitioned in two rays at the middle of pq , and (iii) each half-moon is contained in all disks centered on one of the rays.

In a more general setting, the general idea is (i) to identify a parameter space in \mathbb{R}^k defining the regions, (ii) to partition this space in convex domains, and (iii) have inclusion relations for regions at the vertices of the partition.

The following lemma is instrumental for proving that if a set of region depends on k parameters and if the k -tuple of parameters belongs to a convex polyhedron P of \mathbb{R}^k then, if we want to prove that all regions parameterized by P contain a given region, it is enough to prove this inclusion for the regions parameterized by the vertices of P . If P is not bounded, we can extend the lemma to limit points at infinity: for a point c going

to infinity along some ray of \mathbb{R}^k the region r_c has a limit. The result also holds using this limit regions. We will show below as a didactic example how this lemma can be applied on Delaunay disks.

Lemma 5 (Combination Lemma) *Let $c \in \mathbb{R}^k$ and $E_c : \mathbb{R}^d \rightarrow \mathbb{R}$ such that for any $x \in \mathbb{R}^d$, $c \mapsto E_c(x)$ is an affine function, and let r_c be the region $\{x \in \mathbb{R}^d, E_c(x) < 0\}$. Let P be a subset of \mathbb{R}^k , if $c \in P$, then $\bigcap_{v \in \mathcal{X}(P)} r_v \subset r_c$, where $\mathcal{X}(P)$ denotes the extreme points of the convex hull of P .*

Proof. Consider two points $a, b \in P \subset \mathbb{R}^k$. Let $x \in r_a \cap r_b$ and, for $t \in [0, 1]$, $c_t = (1-t)a + tb$ be a point on $[ab]$. The function $f : t \mapsto E_{c_t}(x)$ verifies $f(0) = E_a(x) < 0$ and $f(1) = E_b(x) < 0$. Since f is affine, for any $t \in [0, 1]$, $E_{c_t}(x) = f(t) = (1-t)f(0) + tf(1) < 0$, so $x \in r_{c_t}$. Thus $r_a \cap r_b \subset r_{c_t}$ for any c_t on the edge $[ab]$. The extension from an edge $[ab]$ to the convex hull of P follows directly from the its convexity. \square

We now show, as an example, that any Delaunay disk contains one of the two half-moons using the Combination lemma:

Corollary 6 *Let p, q two points in the Euclidean plane and D a disk with p and q on its boundary, then $hm_r(p, q) \subset D$ or $hm_\ell(p, q) \subset D$*

Proof. We choose the coordinate system so that p is the origin and $q = (x_q, y_q)$ with $y_q \neq 0$. A disk D with p and q on its boundary can be parameterized by the inequality $E_c(x, y) : x^2 - 2xx_c + y^2 - 2yy_c < 0$ where c verifies $y_c = \frac{x_q^2 - 2x_qx_c + y_q^2}{2y_q}$. Since this is actually the equation of the bisector line of $[pq]$, the centers $c = (x_c, y_c)$ are the actual geometric centers of the disks. That provides a 1-dimensional family of disks parameterized by x_c . In that parameterization, $x_c \mapsto E_c(x, y)$ is an affine function.

Then we can consider the center c_{Gab} of the Gabriel disk and the center c_r at the infinity of the bisector line to the right of \vec{pq} ; their associated regions are the Gabriel disk $\text{Gab}(p, q)$ and the half-plane $hp_r(p, q)$ to the right of \vec{pq} . Since the ray $[c_{\text{Gab}}, c_r)$ is convex, we can apply the Combination lemma with $(k, d) = (1, 2)$ to ensure that any disk whose center belongs to $[c_{\text{Gab}}, c_r)$ contains $hm_r(p, q)$; indeed $hm_r(p, q) = \text{Gab}(p, q) \cap hp_r(p, q)$. We apply the same reasoning for $hm_\ell(p, q)$ to conclude that if a disk has p and q on its boundary, it contains either $hm_r(p, q)$ or $hm_\ell(p, q)$ depending on the position of its center on the bisector line. \square

After the Combination lemma, the second ingredient of our demonstration scheme is the Partition lemma:

Lemma 7 (Partition Lemma) *Let $\mathcal{G}_{\mathcal{R}}^0$ be an empty-region graph with $\mathcal{R}(p, q) = \{r_c; c \in P \subset \mathbb{R}^k\}$ a set of*

regions parameterized by c . Let $(P_i)_{1 \leq i \leq n}$ be a convex subdivision of P , the parameter space. Let $\mathcal{R}_i^(p, q) = \{r_i^*(p, q)\}$ be n singletons. If $\forall c \in P_i; r_i^*(p, q) \subset r_c$ then $\mathcal{G}_{\mathcal{R}}^0$ is a subgraph of $\bigcup_{1 \leq i \leq n} \mathcal{G}_{\mathcal{R}_i^*}^0$ and*

$$\deg(p, \mathcal{G}_{\mathcal{R}}^0) \leq \sum_{1 \leq i \leq n} \deg(p, \mathcal{G}_{\mathcal{R}_i^*}^0).$$

Proof. If pq is an edge of $\mathcal{G}_{\mathcal{R}}^0(X)$, according to Definition 1, there exists $c \in P$ such that $r_c(p, q) \cap X = \emptyset$. Using the convex subdivision, there is some j such that $c \in P_j$ and $r_j^*(p, q) \subset r_c(p, q)$ by the hypothesis in the lemma. Thus $r_j^*(p, q) \cap X = \emptyset$ and pq is also an edge of $\mathcal{G}_{\mathcal{R}_j^*}^0$. \square

Using these two lemmas, the general idea of the method we apply to compute an upper bound on the degree of a point in a given empty-region graph of a Poisson point process can be outlined as follows: (i) find a good affine parameterization of the regions to be able to apply the Combination lemma, (ii) find a good partition of the parameter space to be able to apply the Partition lemma, and (iii) analyze the size of the relevant empty-singleton-region graphs.

4 Empty Axis-Aligned Ellipse Graphs

In this section, we analyze empty-region graphs where the regions are axis-aligned ellipses. By “axis-aligned”, we mean that their axes of symmetry are parallel to the x and y axes. We then call aspect ratio, the ratio of the lengths of the vertical axis to the horizontal axis of the ellipse.

4.1 Some Features of Axis-Aligned Ellipses

We give some explanations on the expression of ellipses we consider, and some properties that will be used thereafter. In \mathbb{R}^2 , we consider an axis-aligned ellipse with the origin p on its boundary. We denote the ellipse r since it is seen as a region. Such an ellipse has three degrees of freedom, that can be set by considering a positive number α and a point $c = (x_c, y_c)$, so that r can be defined by the inequality:

$$r : \alpha^2 x^2 - 2xx_c + y^2 - 2yy_c < 0.$$

In that parameterization, c is the affine parameter of r , and α its aspect ratio. To ensure that the boundary of the ellipse passes through a second point q , the three parameters x_c, y_c and α must satisfy: $\alpha^2 x_q^2 - 2x_q x_c + y_q^2 - 2y_q y_c = 0$. Expressing α in terms of c and q , we define

$$E_c(x, y) := \alpha^2 x_q^2 x^2 - 2xx_c + y^2 - 2yy_c, \quad (1)$$

$$\text{with } \alpha^2 = \frac{2x_q x_c - y_q^2 + 2y_q y_c}{x_q^2}.$$

The inequality $E_c(x, y) < 0$ is an affine parameterization of $r_c(p, q)$, the only axis-aligned ellipse passing through p and q with c for parameter. We stress that c is not the usual geometric center of the ellipse.

In some proofs, we bring the expression back to its canonical form namely $\frac{x^2}{a^2} + \frac{y^2}{b^2} - 1 = 0$, in which the ellipse has aspect ratio $\frac{b}{a}$ and area πab .

Proposition 8 For a given $q \in \mathbb{R}^2$, the parameters c of the ellipses $r_c(p, q)$ with same aspect ratio lie on a line perpendicular to (pq) .

Proof. The aspect ratio is given by the coefficient of x^2 in Equation (1). The set of points $c = (x_c, y_c)$ that yields to a constant aspect ratio defines a line parallel to $\mathcal{L} : xx_q + yy_q = 0$, by multiplying by $\frac{x_q}{2}$ and omitting the constant terms in the expression of α^2 . This line is perpendicular to (pq) . \square

Proposition 9 For a given $q \in \mathbb{R}^2$ and for $\alpha \in \mathbb{R}^+$, consider the ellipse $r_c(p, q)$ parameterized by $c = (\alpha^2 \frac{x_q}{2}, \frac{y_q}{2})$.

The geometric center of $r_c(p, q)$ is the midpoint of $[pq]$, and its area is $\frac{\pi}{4} \left(\alpha x_q^2 + \frac{y_q^2}{\alpha} \right)$.

Proof. Transforming the equation $E_c(x, y) < 0$ of $r_c(p, q)$ we get, its canonical form:

$$\frac{4\alpha^2}{\alpha^2 x_q^2 + y_q^2} \left(x - \frac{x_q}{2}\right)^2 + \frac{4}{\alpha^2 x_q^2 + y_q^2} \left(y - \frac{y_q}{2}\right)^2 - 1 < 0.$$

We identify, with that expression, that $r_c(p, q)$ is the translated copy of an ellipse of center p , and area $\frac{\pi}{4} \left(\alpha x_q^2 + \frac{y_q^2}{\alpha} \right)$ by the vector $\frac{1}{2} \vec{pq}$. Details can be found in appendix. \square

4.2 Unbounded Aspect Ratio: Right-Triangle Graph

In this section, we prove, using our framework, a logarithmic bound for the empty axis-aligned ellipse graph of a Poisson point process in a bounded domain. A similar result was proven for a uniform distribution instead of a Poisson distribution [4].

For two points p and q in \mathbb{R}^2 , we consider the family $Ell(p, q)$ of all axis-aligned ellipses with p and q on their boundaries. Assuming that p is the origin, we show that the expected degree of p in the associated empty-region graph $\mathcal{G}_{Ell}^0(X)$ is $\Theta(\ln \lambda)$ when X is a Poisson process of intensity λ . In order to identify an upper bound, we consider the graph $\mathcal{G}_{\{\Delta_r, \Delta_\ell\}}^0$ where $\Delta_r(p, q)$ (resp. $\Delta_\ell(p, q)$) denotes the axis-aligned right triangle with hypotenuse $[pq]$ on the right (resp. left) side of \vec{pq} .

Lemma 10 $\mathcal{G}_{\{\Delta_r, \Delta_\ell\}}^0$ is a super-graph of \mathcal{G}_{Ell}^0 .

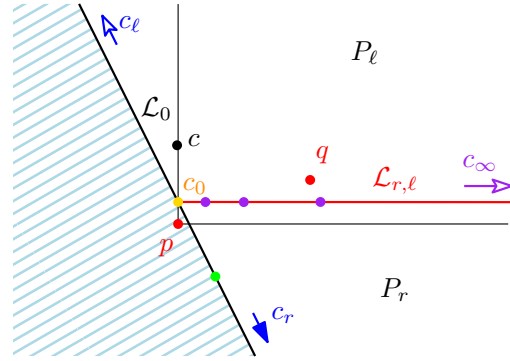


Figure 2: Partition of space of parameters into $\{P_\ell, P_r\}$.

Proof. For each region $r_c(p, q) \in Ell(p, q)$, we consider the parameterization $r_c(p, q) : E_c(x, y) < 0$ where E_c is defined in Equation (1).

The space $P \subset \mathbb{R}^2$ where c lives is delimited by the inequality: $2x_q x_c - y_q^2 + 2y_q y_c > 0$ that is the half-plane whose boundary is the line \mathcal{L}_0 perpendicular to (pq) passing through $c_0 = (0, \frac{y_q}{2})$ and that does not contain p (if c is not in this half-plane, the equation for α^2 has no positive solutions). With a small abuse of notation, we define two points at infinity at the two extremities of \mathcal{L}_0 : c_r to the right of \vec{pq} and c_ℓ to its left. (see Figure 2). On the boundary \mathcal{L}_0 of P , elliptic regions degenerate into parabolas. At point c_0 it degenerates to the horizontal strip $r_{c_0} = \{|y - \frac{y_q}{2}| < \frac{|y_q|}{2}\}$ that can be seen as an ellipse with aspect ratio 0 (see Figure 3). At the limit when going at infinity along \mathcal{L}_0 the parabola degenerates in two half-planes: r_{c_r} and r_{c_ℓ} bounded by (pq) .

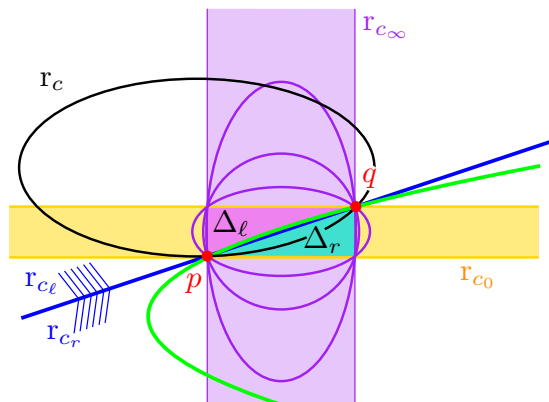


Figure 3: Ellipses corresponding to points in Figure 2. They all contain either Δ_r or Δ_ℓ . Regions whose parameter are on $\mathcal{L}_{r,\ell}$ are in purple, they range from r_{c_0} (in yellow), to r_{c_∞} . Any region whose parameter is in P_ℓ , like r_c , contains Δ_ℓ .

Then, we consider the ray $\mathcal{L}_{r,\ell} : y = \frac{y_q}{2} \cap P$, starting at c_0 , named after the fact that it will distinguish right and left regions. Let c_∞ be the point at infinity on this ray. When the parameter c is equal to c_∞ , the ellipse degenerates into the vertical strip $r_{c_\infty} = \{|x - \frac{x_q}{2}| < \frac{|x_q|}{2}\}$, seen as a vertical ellipse with infinite aspect ratio. For c on $\mathcal{L}_{r,\ell}$, ellipses are centered on the midpoint of $[pq]$ and ranges from the horizontal strip r_{c_0} to the vertical strip r_{c_∞} .

By the Combination lemma, if $c \in P_r$ then

$$\Delta_r = r_{c_0} \cap r_{c_r} \cap r_{c_\infty} \subset r_c$$

and if $c \in P_\ell$ then

$$\Delta_\ell = r_{c_0} \cap r_{c_\ell} \cap r_{c_\infty} \subset r_c.$$

This ensures, by the Partition lemma, that

$$\mathcal{G}_{EU}^\emptyset \subset \mathcal{G}_{\{\Delta_r, \Delta_\ell\}}^\emptyset = \mathcal{G}_{\{\Delta_r\}}^\emptyset(X) \cup \mathcal{G}_{\{\Delta_\ell\}}^\emptyset(X). \quad \square$$

Now, we bound from above the expected degree of p in $\mathcal{G}_{\{\Delta_r\}}^\emptyset(X)$ or $\mathcal{G}_{\{\Delta_\ell\}}^\emptyset(X)$ when X is a Poisson point process with intensity λ .

The area of both triangles Δ_r and Δ_ℓ is $\frac{|x_q y_q|}{2}$. Unfortunately, for any positive λ , $\int_{\mathbb{R}} \int_{\mathbb{R}} e^{-\lambda|xy|} dy dx$ does not converge. In that case, we assume that X is distributed in a rectangle $\mathcal{D} = [-L, L] \times [-l, l]$ for positive L and l .

Lemma 11 *Let X be a Poisson point process with intensity λ in $\mathcal{D} = [-L, L] \times [-l, l]$. The expected degree $\mathbb{E} \left[\deg \left(p, \mathcal{G}_{\{\Delta_r\}}^\emptyset \right) \right]$ of the origin p in $\mathcal{G}_{\{\Delta_r\}}^\emptyset(X)$ is $\Theta(\ln \lambda + \ln L + \ln l)$.*

Proof. Let t be a positive number such that $tLl > 1$, we start by bounding from above the following integral:

$$\begin{aligned} I_{L,l}(t) &= \int_0^L \int_0^l e^{-txy} dy dx \\ &= \int_0^L \int_0^{lx} \frac{e^{-tu}}{x} du dx && \text{with } u = xy \\ &= \int_0^L \frac{1 - e^{-tlx}}{tx} dx \\ &= \frac{1}{t} \int_0^{tLl} \frac{1 - e^{-v}}{v} dv && \text{with } v = tlx \\ &= \frac{1}{t} \left(\int_0^1 \frac{1 - e^{-v}}{v} dv + \int_1^{tLl} \frac{1 - e^{-v}}{v} dv \right) \\ &\leq \frac{1}{t} \left(\int_0^1 dv + \int_1^{tLl} \frac{1}{v} dv \right) \quad \text{since } 1 - e^{-v} \leq \min(1, v) \\ &= \frac{1}{t} (1 + \ln(tLl)). \end{aligned}$$

And bounding from below:

$$\begin{aligned} I_{L,l}(t) &= \frac{1}{t} \int_0^{tLl} \frac{1 - e^{-v}}{v} dv \\ &\geq \frac{1}{t} \int_0^{tLl} \frac{1}{v+1} dv && \text{since } \frac{1 - e^{-v}}{v} \geq \frac{1}{v+1} \text{ if } v \geq 0 \\ &= \frac{1}{t} (\ln(tLl + 1)) &> \frac{\ln(tLl)}{t}. \end{aligned}$$

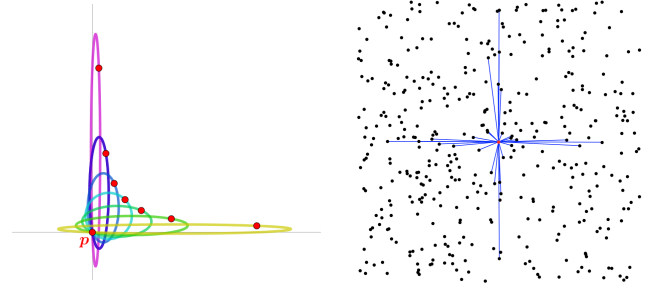


Figure 4: Left: Some xy -ell ellipses whose color depends of the aspect ratio. Right: An instance of $\mathcal{G}_{\{xy\text{-ell}\}}^\emptyset$ where p is the central (red) point. For any point q , xy -ell(p, q) has the smallest area among ellipses passing through p and q so that a far point keeps chance to be a neighbor of p as long as it is close to an axis.

Then we can give an upper bound on the expected degree:

$$\begin{aligned} \mathbb{E} \left[\deg \left(p, \mathcal{G}_{\{\Delta_r\}}^\emptyset \right) \right] &= \mathbb{E} \left[\sum_{q \in X} \mathbb{1}_{[\Delta_r(q) \cap X = \emptyset]} \right] \\ &= \int_{\mathcal{D}} \lambda (\mathbb{P} [\Delta_r(q) \cap X = \emptyset]) dq \\ &= \int_{-L}^L \int_{-l}^l \lambda e^{-\lambda |\Delta_r(q)|} dy dx \\ &= 4\lambda \int_0^L \int_0^l e^{-\lambda \frac{xy}{2}} dy dx \\ &= 4\lambda I_{L,l} \left(\frac{\lambda}{2} \right) = \Theta(\ln(\lambda Ll)). \quad \square \end{aligned}$$

We can compare with the Delaunay triangulation, the Gabriel and the half-moon graphs. In those cases, the empty region had an area quadratic in the distance pq and the expected degree was constant. In this new case, the “ xy ” area provides a logarithmic degree.

Lemmas 10 and 11 give an upper bound on the degree of a point in the empty-axis aligned-ellipse graph. To get a lower bound, we will exhibit a subgraph of $\mathcal{G}_{EU}^\emptyset$. In order to get a tight bound, the area of the chosen region must be $\Theta(x_q y_q)$.

To find such an ellipse, that we name xy -ell(p, q), we use Proposition 9, with $\alpha = \frac{y_q}{x_q}$. We define xy -ell(p, q) to be the ellipse parameterized by $c_{xy} = \left(\frac{y_q}{2x_q}, \frac{y_q}{2} \right)$ (see Figure 4), then according to Proposition 9, the area of this ellipse is $\frac{\pi}{2} x_q y_q$.

Lemma 12 $\mathcal{G}_{\{xy\text{-ell}\}}^\emptyset$ is a subgraph of $\mathcal{G}_{EU}^\emptyset$.

Proof. Straightforward because xy -ell \in Ell. \square

Lemma 13 *Let X be a Poisson point process with intensity λ in $\mathcal{D} = [-L, L] \times [-l, l]$. The expected degree*

$\mathbb{E} \left[\deg \left(p, \mathcal{G}_{\{xy-ell\}}^\theta \right) \right]$ of the origin p in $\mathcal{G}_{\{xy-ell\}}^\theta(X)$ is $\Theta(\ln \lambda + \ln L + \ln l)$.

Proof. As said above, for any $q \in \mathbb{R}^2$, the area of $xy-ell(p, q)$ is $\frac{\pi}{2} x_q y_q$.

Then we can express the expected degree:

$$\begin{aligned} \mathbb{E} \left[\deg \left(p, \mathcal{G}_{\{xy-ell\}}^\theta \right) \right] &= \mathbb{E} \left[\sum_{q \in X} \mathbb{1}_{\{xy-ell(p,q) \cap X = \emptyset\}} \right] \\ &= \int_{\mathcal{D}} \lambda e^{-\lambda |xy-ell(p,q)|} dp \\ &= 4\lambda \int_0^L \int_0^l e^{-\lambda \pi \frac{xy}{2}} dy dx \\ &= \Theta(\ln(\lambda Ll)). \quad \square \end{aligned}$$

The above lemmas allow to conclude:

Theorem 14 Let X be a Poisson point process with intensity λ in $\mathcal{D} = [-L, L] \times [-l, l]$ and p the origin:

$$\mathbb{E} \left[\deg \left(p, \mathcal{G}_{Ell}^\theta \right) \right] = \Theta(\ln \lambda + \ln L + \ln l).$$

4.3 Bounded Aspect Ratio: Rhombus Graph

In the previous part, we proved that when the aspect ratio is not bounded, neither is the expected degree. One can wonder what happens when the aspect ratio ranges between two finite numbers. For two points p and q in \mathbb{R}^2 and a number $\beta \in (0, 1)$, we consider the family $Ell^{[\beta,1]}(p, q)$ of horizontal elliptic regions with p and q on their boundary and whose aspect ratio ranges between β and 1. An important fact to be considered is that, when the aspect ratio is not bounded, a point q far from p could be a neighbor of p as long as it is close enough to the axis, since in that case, ellipses passing through p and q may have a small area, and that leads to a logarithmic bound. When the aspect ratio is bounded, all ellipses preserve an area $\Omega(x_q^2 + y_q^2)$, so that we expect a constant bound on the expected degree. In this section we will prove that it is actually the case and detail how this constant depends on β .

In order to apply the same method as above, we search for simple geometrical regions that fit inside the whole family $Ell^{[\beta,1]}(p, q)$. A good choice is the following: as before, we consider the intersection of ellipses that are centered on the midpoint of $[pq]$, and we cut the intersection along (pq) . The remaining regions $hm_r^{[\beta,1]}(p, q)$ and $hm_\ell^{[\beta,1]}(p, q)$ look like two axis-aligned right triangles with rounded sides for almost all q (see above figure).

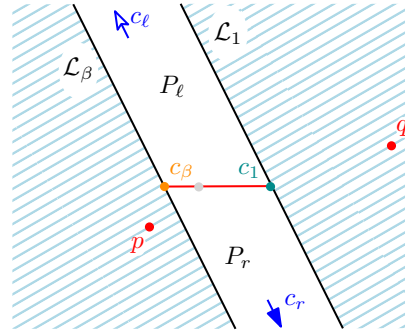
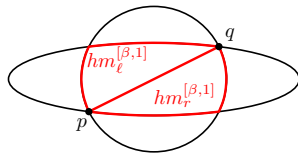


Figure 5: Partition of space of parameters into $\{P_\ell, P_r\}$ in the bounded aspect ratio case.

Lemma 15 The graph $\mathcal{G}_{\{hm_\ell^{[\beta,1]}, hm_r^{[\beta,1]}\}}^\theta$ is a super-graph of $\mathcal{G}_{Ell^{[\beta,1]}}^\theta$.

Proof. The proof is very similar to the one of Lemma 10, so we just spell out the important points. For each $r_c(p, q) \in Ell^{[\beta,1]}(p, q)$, we consider the parameterization $r_c(p, q) : E_c(x, y) < 0$ defined in Equation (1) with $\beta \leq \alpha \leq 1$.

The space $P \subset \mathbb{R}^2$ where c lives is delimited by the inequality: $\beta^2 \leq \frac{2x_q x_c - y_q^2 + 2y_q y_c}{x_q^2} \leq 1$ that is the strip perpendicular to (pq) whose boundary are the lines \mathcal{L}_β and \mathcal{L}_1 , where $\mathcal{L}_\alpha = \{(x, y), \alpha^2 x^2 = 2x_q x - y_q^2 + 2y_q y\}$. We consider the segment defined by $y = \frac{y_q}{2}$ inside P and its extremities c_β on \mathcal{L}_β and c_1 on \mathcal{L}_1 . We partition P into P_r and P_ℓ where P_r is the part of P on the right of $[c_\beta, c_1]$, and P_ℓ the part on its left (see Figure 5).

c_β and c_1 have for regions the ellipses r_{c_β} and r_{c_1} with respectively β and 1 for aspect ratio. Furthermore, any parameter c_r in P at infinity on the right of \vec{pq} has its region that degenerates into the half-plane bounded by (pq) on the right side of \vec{pq} (and the same holds for c_ℓ and the left side).

By the Combination lemma, if $c \in P_r$ then $hm_r^{[\beta,1]} := r_{c_1} \cap r_{c_\beta} \cap r_{c_r} \subset r_c$ and if $c \in P_\ell$ then $hm_\ell^{[\beta,1]} := r_{c_1} \cap r_{c_\beta} \cap r_{c_\ell} \subset r_c$ (see Figure 6). By the Partition lemma, an edge of $\mathcal{G}_{Ell^{[\beta,1]}}^\theta$ is an edge of $\mathcal{G}_{hm_\ell^{[\beta,1]}}^\theta$ or $\mathcal{G}_{hm_r^{[\beta,1]}}^\theta$. \square

The problem now is that it may be complicated to compute an integral involving the area of $hm_r^{[\beta,1]}(p, q)$ or $hm_\ell^{[\beta,1]}(p, q)$. To solve this issue, we consider a strictly smaller region. We could have used the axis-aligned right triangles Δ_r and Δ_ℓ but their areas do not respect the order of magnitude (as illustrated by Figure 7). A more suitable region is what we call the half-rhombus. We define the rhombus $Rh^\beta(p, q)$ as the one whose vertices are the horizontal extreme points of $r_{c_1}(p, q)$ and the vertical extreme points of $r_{c_\beta}(p, q)$. Then we separate it into two halves $Rh_r^\beta(p, q)$ and $Rh_\ell^\beta(p, q)$, delimited by (pq) . By convexity, it is clear that $Rh_r^\beta(p, q) \subset$

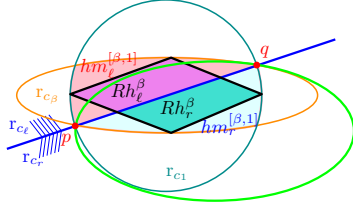


Figure 6: The green ellipse with parameter to the right of \vec{pq} contains Rh_r^β .

$hm_r^{[\beta,1]}(p, q)$ and $Rh_\ell^\beta(p, q) \subset hm_\ell^{[\beta,1]}(p, q)$ (see Figure 6). Finally, we can say that $\mathcal{G}_{\{Rh_r^\beta\}}^\theta$ is a super-graph of $\mathcal{G}_{\{hm_r^{[\beta,1]}\}}^\theta$ and that $\mathcal{G}_{\{Rh_\ell^\beta\}}^\theta$ is a super-graph of $\mathcal{G}_{\{hm_\ell^{[\beta,1]}\}}^\theta$.

Before proceeding to the computation of the expected degree, we introduce a lemma that provides properties on the involved integral.

Lemma 16 Let $t > 0$, $\beta \in (0, 1)$ and

$$I_\beta(t) = \int_{\mathbb{R}} \int_{\mathbb{R}} e^{-t\sqrt{(x^2+y^2)(\beta^2x^2+y^2)}} dy dx,$$

$$I_\beta(t) = \frac{1}{t} I_\beta(1) \leq \frac{\pi}{t} \left(1 + \ln\left(\frac{1}{\beta}\right)\right).$$

Proof. The computations are in appendix. \square

Lemma 17 Let X be a Poisson point process with intensity λ in \mathbb{R}^2 , and $\beta \in (0, 1)$.

$$\mathbb{E} \left[\deg \left(p, \mathcal{G}_{\{Rh_r^\beta\}}^\theta \right) \right] = O\left(\ln \frac{1}{\beta}\right).$$

Proof. We first compute the area of the rhombus $Rh_r^\beta(p, q)$. We identify its width and height as being respectively $\sqrt{x_q^2 + y_q^2}$ and $\sqrt{\beta^2 x_q^2 + y_q^2}$ so that the value of its area is given by $\frac{1}{2} \sqrt{(x_q^2 + y_q^2)(\beta^2 x_q^2 + y_q^2)}$.

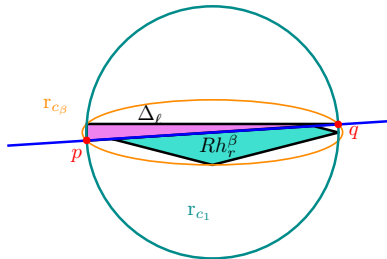


Figure 7: The area of Δ_r and Rh_r^β can have different order of magnitude.

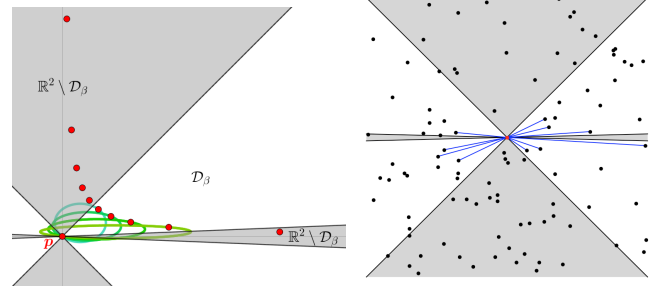


Figure 8: Some β -ellipses for points in \mathcal{D}_β and an instance of $\mathcal{G}_{\{\beta\text{-ell}\}}^\theta$ where p is the red point. A far point reduces strongly its probability to be a neighbor of p because it cannot anymore be close to the axes.

Then we can compute the expected degree of p in $\mathcal{G}_{\{Rh_r^\beta\}}^\theta(X)$:

$$\begin{aligned} \mathbb{E} \left[\deg \left(p, \mathcal{G}_{\{Rh_r^\beta\}}^\theta \right) \right] &= \mathbb{E} \left[\sum_{q \in X} \mathbb{1}_{[Rh_r^\beta(p, q) \cap X = \emptyset]} \right] \\ &= \int_{\mathbb{R}^2} \lambda \mathbb{P} [Rh_r^\beta(p, q) \cap X = \emptyset] \\ &= \int_{\mathbb{R}^2} \lambda e^{-\lambda \frac{1}{2} |Rh_r^\beta(p, q)|} dq \\ &= \int_{\mathbb{R}} \int_{\mathbb{R}} \lambda e^{-\frac{\lambda}{2} \sqrt{(x_q^2 + y_q^2)(\beta^2 x_q^2 + y_q^2)}} dy dx \\ &= \lambda I_\beta \left(\frac{\lambda}{2} \right) \\ &\leq 4\pi (1 - \ln(\beta)) \quad \text{by Lemma 16.} \quad \square \end{aligned}$$

We obtain a tight lower bound, when β goes to 0, by identifying, for each q , a particular region, named $\beta\text{-ell}(p, q)$, such that $\beta\text{-ell}(p, q)$ is or contains an element of $Ell^{[\beta,1]}(p, q)$. To achieve this, we partition the plane into two parts (see Figure 8):

1. if $q \in \mathcal{D}_\beta := \{(x, y), \beta|x| < |y| < |x|\}$, then, as in Lemma 12, we define $\beta\text{-ell}(p, q) = xy\text{-ell}(p, q)$,
2. otherwise $\beta\text{-ell}(p, q) = \mathbb{R}^2$, that is another way to say that q is not a neighbor of p .

Lemma 18 $\mathcal{G}_{\{\beta\text{-ell}\}}^\theta$ is a subgraph of $\mathcal{G}_{\{Ell^{[\beta,1]}\}}^\theta$.

Proof. If $q \in \mathcal{D}_\beta$, we have to prove that $\beta\text{-ell}(p, q)$, i.e. $xy\text{-ell}(p, q)$, is in $Ell^{[\beta,1]}$. This is true because the aspect ratio of if $xy\text{-ell}(p, q)$ is $|\frac{y_q}{x_q}|$, and verifies $\beta < |\frac{y_q}{x_q}| < 1$ if $\beta|x_q| < |y_q| < |x_q|$.

Otherwise, it is clear that $\beta\text{-ell}(p, q)$, i.e. \mathbb{R}^2 , is larger than any other ellipse from $Ell^{[\beta,1]}$. \square

Lemma 19 Let X be a Poisson point process with intensity λ in \mathbb{R}^2 . The expected degree

$\mathbb{E} \left[\deg \left(p, \mathcal{G}_{\{\beta\text{-ell}\}}^\emptyset \right) \right]$ of the origin p in $\mathcal{G}_{\{\beta\text{-ell}\}}^\emptyset(X)$ is $\Theta(\ln \frac{1}{\beta})$.

Proof. $\beta\text{-ell}(p, q)$ is actually chosen to simplify the computation. Recall that \mathcal{D}_β is the domain $\{(x, y), \beta|x| < |y| < |x|\}$;

$$\begin{aligned}
 \mathbb{E} \left[\deg \left(p, \mathcal{G}_{\{\beta\text{-ell}\}}^\emptyset \right) \right] &= \mathbb{E} \left[\sum_{q \in X} \mathbb{1}_{[\beta\text{-ell}(p, q) \cap X = \emptyset]} \right] \\
 &= \int_{\mathbb{R}^2} \lambda \mathbb{P} [\beta\text{-ell}(p, q) \cap X = \emptyset] dp \\
 &= \int_{\mathcal{D}_\beta} \lambda \mathbb{P} [xy\text{-ell}(p, q) \cap X = \emptyset] dp + \int_{\mathbb{R}^2 \setminus \mathcal{D}_\beta} 0 dp \\
 &= \int_{\mathcal{D}_\beta} \lambda e^{-\lambda |xy\text{-ell}(p, q)|} dp \\
 &= 4 \int_0^\infty \int_{\beta x}^x \lambda e^{-\lambda \pi \frac{xy}{2}} dy dx \\
 &= 4 \int_{\tan^{-1}(\beta)}^{\frac{\pi}{4}} \int_0^\infty \lambda \rho e^{-\lambda \pi \frac{\rho^2 \cos(\theta) \sin(\theta)}{2}} d\rho d\theta \\
 &= 4 \int_{\tan^{-1}(\beta)}^{\frac{\pi}{4}} \lambda \frac{1}{\lambda \pi \cos(\theta) \sin(\theta)} d\theta \\
 &= \frac{4}{\pi} (\ln(\tan(\frac{\pi}{4})) - \ln(\beta)) \quad \text{since } \frac{d}{d\theta} \ln(\tan(\theta)) = \frac{1}{\cos(\theta) \sin(\theta)} \\
 &= \frac{4}{\pi} \ln(\frac{1}{\beta}). \quad \square
 \end{aligned}$$

We can finally conclude using Lemmas 15 to 19:

Theorem 20 Let X be a Poisson point process with intensity λ in \mathbb{R}^2 . The expected degree $\mathbb{E} [\deg (p, \mathcal{G}_{Ell[\beta, 1]}^\emptyset)]$ of the origin p in $\mathcal{G}_{Ell[\beta, 1]}^\emptyset(X \cup \{p\})$ is $\Theta \left(\ln(\frac{1}{\beta}) \right)$.

If $\beta > 1$ we have by symmetry,

$$\mathbb{E} \left[\deg \left(p, \mathcal{G}_{Ell[1, \beta]}^\emptyset \right) \right] = \mathbb{E} \left[\deg \left(p, \mathcal{G}_{Ell[\frac{1}{\beta}, 1]}^\emptyset \right) \right] = \Theta(\ln \beta).$$

4.4 Non-Axis-Aligned Ellipses

We turn our interest to the case of non-axis-aligned ellipses. We consider the graph in which two points p and q are neighbors if there exists an empty ellipse passing through p and q whose aspect ratio is between β and 1, for $\beta \in [0, 1]$. For two points p and q , we define the family $Ell_*^{[\beta, 1]}(p, q)$ of all ellipses with such aspect ratios passing through p and q , and $\mathcal{G}_{Ell_*^{[\beta, 1]}}^\emptyset$, the corresponding empty region graph.

The case where $\beta = 1$ corresponds to the Delaunay triangulation, and the case where $\beta = 0$ corresponds to the complete graph, since we can consider that a segment between two points is an ellipse with aspect ratio 0 and random points are in general position. Thus we assume that $\beta \in (0, 1)$.

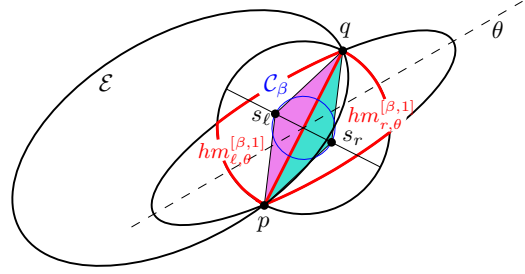


Figure 9: Non-axis-aligned ellipses.

Consider two points, p at the origin and q , and an ellipse \mathcal{E} passing through p and q . Since \mathcal{E} is not anymore axis-aligned but has its great axis in some direction θ , we can consider the regions $hm_{r, \theta}^{[\beta, 1]}$ and $hm_{l, \theta}^{[\beta, 1]}$ as in the previous sections but parameterized by direction θ . Clearly the circle \mathcal{C}_β centered at the midpoint of pq and of diameter $\beta|pq|$ is inside $hm_{r, \theta}^{[\beta, 1]} \cup hm_{l, \theta}^{[\beta, 1]}$ (see Figure 9). Consider the isosceles triangles pqs_r and pqs_l such that $s_\ell, s_r \in \mathcal{C}_\beta$ with s_r on the right of \vec{pq} and s_ℓ on its left. Then $pqs_r \subset hm_{r, \theta}^{[\beta, 1]}$ and $pqs_l \subset hm_{l, \theta}^{[\beta, 1]}$.

Since this is true for any ellipse, we can assume that any ellipse whose aspect ratio is between β and 1 and passing through p and q contains either pqs_r or pqs_l . Notice that these triangles are independent of the direction θ . So we can apply the Partition lemma to yield that $\mathcal{G}_{Ell_*^{[\beta, 1]}}^\emptyset$ is a subgraph of $\mathcal{G}_{\{pqs_r, pqs_l\}}^\emptyset$.

Now we consider a Poisson point process X of intensity λ , and we compute an upper bound on the expected degree of p in $\mathcal{G}_{Ell_*^{[\beta, 1]}}^\emptyset(X \cup \{p\})$.

$$\begin{aligned}
 &\mathbb{E} \left[\deg \left(p, \mathcal{G}_{\{pqs_r, pqs_l\}}^\emptyset \right) \right] \\
 &\leq 2 \mathbb{E} \left[\sum_{q \in X} \mathbb{1}_{[pqs_r \cap X = \emptyset]} \right] \\
 &= 2 \int_{\mathbb{R}^2} \lambda \mathbb{P} [pqs_r \cap X = \emptyset] dq \\
 &= 2 \int_{\mathbb{R}^2} \lambda e^{-\lambda |pqs_r|} dq \\
 &= 2 \int_0^{2\pi} \int_0^\infty \lambda e^{-\frac{\lambda}{8} \beta \rho^2} \rho d\rho d\theta = \frac{16\pi}{\beta}.
 \end{aligned}$$

On the other hand, among the ellipses passing through p and q , we can choose the ellipse \mathcal{E}_{β^*} whose great axis is $[p, q]$ and has aspect ratio β to obtain a subgraph of $\mathcal{G}_{Ell_*^{[\beta, 1]}}^\emptyset$.

The expected degree of p in this graph is

$$\begin{aligned} \mathbb{E} \left[\deg \left(p, \mathcal{G}_{\{\mathcal{E}_{\beta^*}\}}^0 \right) \right] &= \mathbb{E} \left[\sum_{q \in X} \mathbb{1}_{[\mathcal{E}_{\beta^*} \cap X = \emptyset]} \right] \\ &= \int_{\mathbb{R}^2} \lambda \mathbb{P} [\mathcal{E}_{\beta^*} \cap X = \emptyset] dq \\ &= \int_{\mathbb{R}^2} \lambda e^{-\lambda |\mathcal{E}_{\beta^*}|} dq \\ &= \int_0^{2\pi} \int_0^\infty \lambda e^{-\lambda \frac{\pi}{4} \beta \rho^2} \rho d\rho d\theta = \frac{4}{\beta} \end{aligned}$$

We deduce the following theorem:

Theorem 21 *Let X be a Poisson point process in \mathbb{R}^2 . The expected degree of the origin p in $\mathcal{G}_{EU_*^{[\beta,1]}}^0(X \cup \{p\})$ is $\Theta \left(\frac{1}{\beta} \right)$.*

5 Probability of Existence of Far Neighbors

At some point, for a given graph \mathcal{G} and a positive number t , we may be interested in computing the probability for p to have a neighbor in \mathcal{G} at a distance greater than t .

As before, for illustration on a simple case, we start by the Delaunay triangulation:

Lemma 22 *Let X be a Poisson point process with intensity λ in \mathbb{R}^2 , p a point of \mathbb{R}^2 , and t a positive number. The probability that p has some Delaunay neighbor at a distance greater than t is smaller than $8e^{-\lambda \frac{\sqrt{2}}{8} t^2}$.*

Proof. If q is a Delaunay neighbor of p , Let σ be an empty disk whose boundary passes through p and q . If q is at distance greater than t from p , then the diameter of σ is obviously also greater than t , so its homothet σ' toward p that has exactly diameter t is included in σ and by consequence empty.

Consider the triangle with vertices p , $(\frac{\sqrt{2}}{2}t, 0)$, and $(\frac{1}{2}t, \frac{1}{2}t)$ and its seven adjacent copies around p (see Figure 10). We name them τ_i for $i \in \{1, \dots, 8\}$. Their area is $|\tau_1| = \frac{\sqrt{2}}{8}t^2$.

One can notice that, at least one triangle is included in σ' : the one whose angular sector from p contains the center of σ' .

So we get:

$$\begin{aligned} &\mathbb{P} [\exists q \in X; [pq] \in \text{Del}(X \cup \{p\}) \mid |pq| > t] \\ &\leq \mathbb{P} [\exists i \in [1, \dots, 8], \tau_i \cap X = \emptyset] \\ &\leq \sum_{i=1, \dots, 8} \mathbb{P} [\tau_i \cap X = \emptyset] \\ &= 8 \mathbb{P} [\tau_1 \cap X = \emptyset] = 8e^{-\lambda \frac{\sqrt{2}}{8} t^2}. \quad \square \end{aligned}$$

We establish in the next lemma a similar bound for the empty axis-aligned ellipse graph with bounded aspect ratio in $[\beta, 1]$. We are mainly interested in the behavior of the probability when β is small, thus we assume $\beta < \frac{1}{2}$.

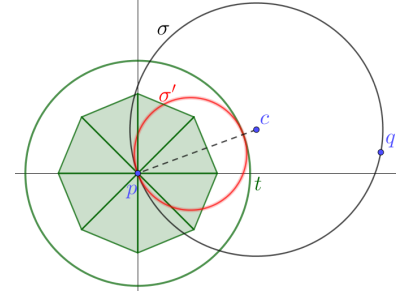


Figure 10: If $|pq| > t$, any disk passing through p and q contains one of the 8 triangles.

Lemma 23 *Let X be a Poisson point process with intensity λ in \mathbb{R}^2 , p a point of \mathbb{R}^2 , t and β two positive numbers with $\beta < \frac{1}{2}$. The probability that p has some neighbor in $\mathcal{G}_{EU^{[\beta,1]}}^0(X)$ at a distance greater than t is smaller than $4 \left(e^{-\lambda \frac{\sqrt{2}}{16} \beta t^2} + e^{-\lambda \frac{\sqrt{2}}{16} \beta^{\frac{3}{2}} t^2} \right)$.*

Proof. The proof idea is similar to the previous one, except that we apply a homothety on the empty ellipse σ until its image σ' fits inside the axis-aligned square inscribed in the circle of radius t (see Figure 11).

We consider eight triangles $(tr_i)_{1 \leq i \leq 8}$, that have the property that for any ellipse σ , σ' contains one of them.

To this aim we define the four points

$$\begin{aligned} v_1 &= (\frac{1}{2}t, 0), & v_2 &= (\frac{\sqrt{2}}{4}t, \frac{\sqrt{2}}{4}\beta t), \\ v_3 &= (\frac{\sqrt{2}\beta}{4}t, \frac{\sqrt{2}}{4}\beta t), & v_4 &= (0, \frac{1}{2}\beta t). \end{aligned}$$

The triangles tr_1 and tr_2 are respectively pv_1v_2 and pv_3v_4 . Their respective areas are $\frac{\sqrt{2}}{16}\beta t^2$ and $\frac{\sqrt{2}}{16}\beta^{\frac{3}{2}}t^2$. We will show that any ellipse tangent to the square in the upper right quadrant contains tr_1 or tr_2 . We complete the set of triangles by their symmetrical copies with respect to the x -axis, to the y -axis and to the point p , and name them according to the trigonometric order

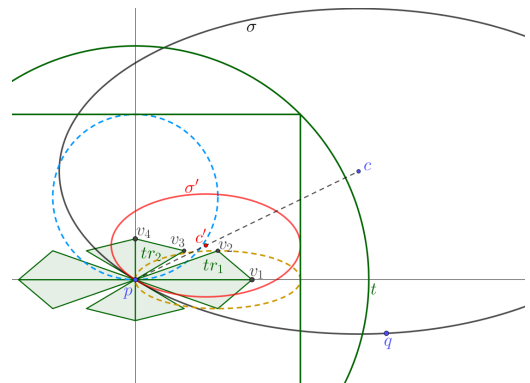


Figure 11: If $|pq| > t$, any ellipse passing through p and q contains one of the 8 triangles.

from tr_1 to tr_8 to cover the ellipses tangent to other parts of the square.

Without loss of generality, we assume that the center c' of σ' is in the upper right quadrant. In such a case, the right most point of σ' has abscissa $\frac{\sqrt{2}}{2}t$, its left most point has negative abscissa, and its center verifies $0 \leq x_{c'} \leq \frac{\sqrt{2}}{4}t$.

As long as $x_{c'} \geq \frac{1}{4}t$, using the symmetry of the ellipse with respect to its vertical axis, v_1 is between p and the symmetric of p , and thus is inside σ_0 . We prove that such ellipses, with $x_{c'} \geq \frac{1}{4}t$, also contain v_2 . Actually v_2 is chosen as the highest point of the thinnest ellipse of center $c' = (\frac{\sqrt{2}}{4}t, 0)$ (in yellow on Figure 11), with aspect ratio β . Since the abscissa of v_2 is between p and v_1 , moving the center c' upward or to the left or increasing β imply that v_2 remains inside σ' . So as long as $x_{c'} \geq \frac{1}{4}t$, the triangle tr_1 is inside σ' .

Suppose now that $x_{c'} \leq \frac{1}{4}t$. The ellipse σ' , if its aspect ratio is α , has equation:

$$\alpha^2 x^2 - 2\alpha^2 x x_{c'} + y^2 - 2y y_{c'} \leq 0.$$

For a fixed α , the lowest possible center is reached when $x_{c'} = \frac{1}{4}t$ and since σ' is tangent to the right side of the square at $(\frac{\sqrt{2}}{2}t, y_{c'})$, by substitution we have:

$$\frac{1}{2}\alpha^2 t^2 - \sqrt{2}\alpha^2 t \frac{1}{4}t - y_{c'}^2 = 0.$$

Thus $y_{c'}$ is minimized for $\alpha = \beta$, and so:

$$y_{c'} = \frac{1}{2}\sqrt{2 - \sqrt{2}}\beta t \simeq 0.383\beta t.$$

We can deduce, by symmetry with respect to the horizontal axis of σ' , that all those ellipses contain the segment between p and $(0, \sqrt{2 - \sqrt{2}}\beta t)$, including v_4 .

To prove that $v_3 \in \sigma'$, we make a distinction between the side of tangency of σ' . We call contact point of an ellipse, the point of the ellipse in which it is tangent to the square, for σ' we name it q' . Suppose first that σ' is tangent to the right side of the square. We consider the two extreme ellipses σ_{high} and σ_{low} , with highest and lowest contact points q_{high} and q_{low} , at respectively $\frac{\sqrt{2}}{4}t$ and $\frac{1}{2}\sqrt{2 - \sqrt{2}}\beta t$ for ordinate. They both contain v_3 :

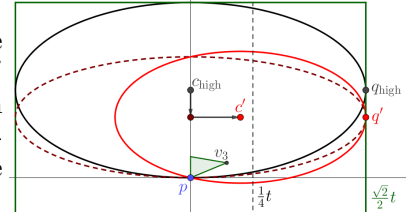
$$\begin{aligned} v_3 \in \sigma_{\text{low}} : \\ \beta^2 \left(\frac{\sqrt{2\beta}}{4}t\right)^2 - \beta^2 \left(\frac{\sqrt{2\beta}}{4}t\right) \frac{1}{4} + \left(\frac{\sqrt{2}}{4}\beta t\right)^2 - 2\left(\frac{\sqrt{2}}{4}\beta t\right) \frac{\sqrt{2-\sqrt{2}}\beta t}{2} \\ = \beta^2 t^2 \left(\frac{\beta}{8} - \frac{\sqrt{2\beta}}{16} + \frac{1}{8} - \frac{\sqrt{4-2\sqrt{2}}}{8}\right) \leq 0 \quad \text{for } \beta \leq 0.6 \end{aligned}$$

$$\begin{aligned} v_3 \in \sigma_{\text{high}} : \\ \left(\frac{\sqrt{2\beta}}{4}t\right)^2 - 0 + \left(\frac{\sqrt{2}}{4}\beta t\right)^2 - 2\left(\frac{\sqrt{2}}{4}\beta t\right) \frac{\sqrt{2}}{4}t \\ = \beta t^2 \left(\frac{1}{8} + \frac{\beta}{8} - \frac{2}{8}\right) \leq 0 \quad \text{since } \beta \leq 1 \end{aligned}$$

We call bottom part of the ellipse, the counterclockwise arc from p to the contact point, and top part the

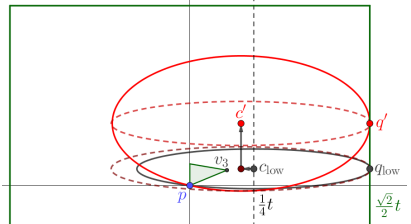
following arc from the contact point to the intersection with the y -axis.

We show that the bottom part of σ' is below the bottom part of σ_{high} . We apply a vertical affine transformation that



flattens σ_{high} until its contact point becomes q' . The new ellipse clearly has its bottom part lower since the transformation lowered every point. Then we shift horizontally the center into c' , maintaining the points p and q' . Since that makes the aspect ratio grow, here again we lowered the bottom part. So the bottom part of σ' is below the bottom part of σ_{high} .

On the other hand we apply a homothetic transformation on σ_{low} centered on its contact point such that the length of the



horizontal axis is the same as the length as σ' , followed by a vertical translation until the contact point coincides with q' , finally completed by a vertical affine transformation that makes it reach the correct aspect ratio, that is greater. All these transformations make the upper part of the ellipse go upward. We deduce that any ellipse tangent to the right side of the square and whose center has abscissa smaller than $\frac{1}{4}t$ contains tr_2 .

Then we can go to ellipses tangent to the top side of the square. The proof is quite identical so we do not develop it but keep in mind that the important point is that v_3 belongs to circle centered at $(0, \frac{\sqrt{2}}{4}t)$ because v_3 lies on the parabola $y = \frac{2\sqrt{2}}{t}x^2$, that is above the circle for $y < \frac{\sqrt{2}}{4}t$.

Above arguments proved that any ellipse whose center is in the upper right corner of the triangle contains either (pv_1v_2) or (pv_3v_4) . By extension, we deduce that any ellipse contains at least one of the 8 triangles tr_i .

So we get:

$$\begin{aligned} & \mathbb{P} \left[[pq] \in \mathcal{G}_{EU[\beta,1]}^\emptyset(X) \mid |pq| > t \right] \\ & \leq \mathbb{P} [\exists i \in [1, \dots, 8], tr_i \cap X = \emptyset] \\ & = 4 (\mathbb{P} [tr_1 \cap X = \emptyset] + \mathbb{P} [tr_2 \cap X = \emptyset]) \\ & = 4 \left(e^{-\lambda \frac{\sqrt{2}}{16}\beta t^2} + e^{-\lambda \frac{\sqrt{2}}{16}\beta \frac{3}{2}t^2} \right) \\ & = \Theta(e^{-\lambda \sqrt{2}\beta \frac{3}{2}(\frac{1}{4}t)^2}) \quad \square \end{aligned}$$

Acknowledgements

The authors thank Sylvain Lazard for its relevant suggestions.

References

- [1] N. Amenta, M. Bern, and D. Eppstein. The crust and the β -skeleton: Combinatorial curve reconstruction. *Graphical models and image processing*, 60(2):125–135, 1998. doi:10.1006/gmip.1998.0465.
- [2] J. Cardinal, S. Collette, and S. Langerman. Empty region graphs. *Computational geometry*, 42(3):183–195, 2009. doi:10.1016/j.comgeo.2008.09.003.
- [3] B. Delaunay et al. Sur la sphere vide. *Izv. Akad. Nauk SSSR, Otdelenie Matematicheskii i Estestvennyka Nauk*, 7(793-800):1–2, 1934.
- [4] O. Devillers, J. Erickson, and X. Goaoc. Empty-ellipse graphs. In *19th Annual ACM-SIAM Symposium on Discrete Algorithms (SODA'08)*, pages 1249–1256, San Francisco, United States, 2008. URL: <https://hal.inria.fr/inria-00176204>.
- [5] L. Devroye, C. Lemaire, and J.-M. Moreau. Expected time analysis for delaunay point location. *Computational geometry*, 29(2):61–89, 2004. doi:10.1016/j.comgeo.2004.02.002.
- [6] K. R. Gabriel and R. R. Sokal. A new statistical approach to geographic variation analysis. *Systematic Biology*, 18(3):259–278, 09 1969. doi:10.2307/2412323.
- [7] D. G. Kirkpatrick and J. D. Radke. A framework for computational morphology. In *Machine Intelligence and Pattern Recognition*, volume 2, pages 217–248. Elsevier, 1985.
- [8] R. Schneider and W. Weil. *Stochastic and Integral Geometry*. Probability and Its Applications. Springer, 2008.
- [9] A. C.-C. Yao. On constructing minimum spanning trees in k-dimensional spaces and related problems. *SIAM Journal on Computing*, 11(4):721–736, 1982. doi:10.1137/0211059.

Appendix

Proof. Integral for Theorem 2

We have to compute

$$\mathbb{E}[\deg(p, \text{Del})] = \frac{1}{2} \int_{\mathbb{R}^2} \int_{\mathbb{R}^2} \lambda^2 e^{-\lambda|D(p,q,r)|} d\mathbf{r}dq.$$

We use a Blaschke-Petkantschin like variables substitution [8, Theorem 7.2.7] from \mathbb{R}^4 to $\mathbb{R}^+ \times [0, 2\pi]^3$, to express the parameterization of q and r into $(\rho, \varphi, \theta_q, \theta_r)$ where (ρ, φ) denotes the polar coordinates of the center c of the circle circumscribing p, q , and r , and θ_q and θ_r denote the angles of the points q and r from c to the horizontal line (see Figure 12).

$$\begin{aligned} x_q &= \rho(\cos \varphi + \cos \theta_q), & y_q &= \rho(\sin \varphi + \sin \theta_q), \\ x_r &= \rho(\cos \varphi + \cos \theta_r), & y_r &= \rho(\sin \varphi + \sin \theta_r). \end{aligned}$$

The Jacobian matrix J of the transformation can be written:

$$J(\rho, \varphi, \theta_q, \theta_r) = \begin{pmatrix} \cos \varphi + \cos \theta_q & -\rho \sin \varphi & -\rho \sin \theta_q & 0 \\ \sin \varphi + \sin \theta_q & \rho \cos \varphi & \rho \cos \theta_q & 0 \\ \cos \varphi + \cos \theta_r & -\rho \sin \varphi & 0 & -\rho \sin \theta_r \\ \sin \varphi + \sin \theta_r & \rho \cos \varphi & 0 & \rho \cos \theta_r \end{pmatrix},$$

and has the following determinant:

$$\begin{aligned} \det(J(\rho, \varphi, \theta_q, \theta_r)) &= \begin{vmatrix} \cos \varphi + \cos \theta_q & -\rho \sin \varphi & -\rho \sin \theta_q & 0 \\ \sin \varphi + \sin \theta_q & \rho \cos \varphi & \rho \cos \theta_q & 0 \\ \cos \varphi + \cos \theta_r & -\rho \sin \varphi & 0 & -\rho \sin \theta_r \\ \sin \varphi + \sin \theta_r & \rho \cos \varphi & 0 & \rho \cos \theta_r \end{vmatrix} \\ &= (\cos \varphi + \cos \theta_q) \begin{vmatrix} \rho \cos \varphi & \rho \cos \theta_q & 0 \\ -\rho \sin \varphi & 0 & -\rho \sin \theta_r \\ \rho \cos \varphi & 0 & \rho \cos \theta_r \end{vmatrix} \\ &\quad - (\sin \varphi + \sin \theta_q) \begin{vmatrix} -\rho \sin \varphi & -\rho \sin \theta_q & 0 \\ -\rho \sin \varphi & 0 & -\rho \sin \theta_r \\ \rho \cos \varphi & 0 & \rho \cos \theta_r \end{vmatrix} \\ &\quad + (\cos \varphi + \cos \theta_r) \begin{vmatrix} -\rho \sin \varphi & -\rho \sin \theta_q & 0 \\ \rho \cos \varphi & \rho \cos \theta_q & 0 \\ \rho \cos \varphi & 0 & \rho \cos \theta_r \end{vmatrix} \\ &\quad - (\sin \varphi + \sin \theta_r) \begin{vmatrix} -\rho \sin \varphi & -\rho \sin \theta_q & 0 \\ \rho \cos \varphi & \rho \cos \theta_q & 0 \\ -\rho \sin \varphi & 0 & -\rho \sin \theta_r \end{vmatrix} \end{aligned}$$

We develop from the coefficient that is the only not zero in a column,

$$\begin{aligned} &= (\cos \varphi + \cos \theta_q) (-\rho \cos \theta_q) (-\rho^2 \sin \varphi \cos \theta_r + \rho^2 \cos \varphi \sin \theta_r) \\ &\quad - (\sin \varphi + \sin \theta_q) (\rho \sin \theta_q) (-\rho^2 \sin \varphi \cos \theta_r + \rho^2 \cos \varphi \sin \theta_r) \\ &\quad + (\cos \varphi + \cos \theta_r) (\rho \cos \theta_r) (-\rho^2 \sin \varphi \cos \theta_q + \rho^2 \cos \varphi \sin \theta_q) \\ &\quad - (\sin \varphi + \sin \theta_r) (-\rho \sin \theta_r) (-\rho^2 \sin \varphi \cos \theta_q + \rho^2 \cos \varphi \sin \theta_q) \\ &= \rho^3 ((-\cos \varphi \cos \theta_q - \cos^2 \theta_q) (-\sin \varphi \cos \theta_r + \cos \varphi \sin \theta_r) \\ &\quad - (\sin \varphi \sin \theta_q + \sin^2 \theta_q) (-\sin \varphi \cos \theta_r + \cos \varphi \sin \theta_r) \\ &\quad + (\cos \varphi \cos \theta_r + \cos^2 \theta_r) (-\sin \varphi \cos \theta_q + \cos \varphi \sin \theta_q) \\ &\quad - (-\sin \varphi \sin \theta_r - \sin^2 \theta_r) (-\sin \varphi \cos \theta_q + \cos \varphi \sin \theta_q)). \end{aligned}$$

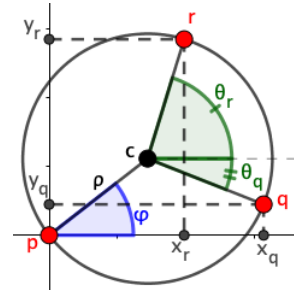


Figure 12: The Blaschke-Petkantschin variables substitution converts the Cartesian coordinates of q and r into polar coordinates related to the circle circumscribing p, q and r .

We factorize by the right factor,

$$\begin{aligned} &= \rho^3 \left((-\cos \varphi \cos \theta_q - \cos^2 \theta_q - \sin \varphi \sin \theta_q - \sin^2 \theta_q) \right. \\ &\quad \cdot (-\sin \varphi \cos \theta_r + \cos \varphi \sin \theta_r) \\ &\quad + (\cos \varphi \cos \theta_r + \cos^2 \theta_r + \sin \varphi \sin \theta_r + \sin^2 \theta_r) \\ &\quad \cdot (-\sin \varphi \cos \theta_q + \cos \varphi \sin \theta_q) \left. \right) \\ &= \rho^3 \left((-\cos \varphi \cos \theta_q - \sin \varphi \sin \theta_q - 1) (-\sin \varphi \cos \theta_r + \cos \varphi \sin \theta_r) \right. \\ &\quad \left. + (\cos \varphi \cos \theta_r + \sin \varphi \sin \theta_r + 1) (-\sin \varphi \cos \theta_q + \cos \varphi \sin \theta_q) \right). \end{aligned}$$

We distribute the 1, develop, and many terms cancel each other,

$$\begin{aligned} &= \rho^3 \left(\sin \theta_q \cos \theta_r - \cos \theta_q \sin \theta_r + \sin \varphi \cos \theta_r \right. \\ &\quad \left. - \cos \varphi \sin \theta_r - \sin \varphi \cos \theta_q + \cos \varphi \sin \theta_q \right). \end{aligned}$$

Finally we apply the formulae: $\cos a \sin b - \cos b \sin a = \sin(a - b)$, on the three well-chosen pairs of terms,

$$\begin{aligned} &= \rho^3 (\sin(\theta_q - \theta_r) + \sin(\theta_q - \varphi) + \sin(\varphi - \theta_r)) \\ &= \rho^3 (\sin(\pi - (\theta_q - \theta_r)) + \sin(\theta_q - \varphi) + \sin(\varphi - \theta_r)) \\ &= 4\rho^3 \sin\left(\frac{\pi - (\theta_q - \theta_r)}{2}\right) \sin\left(\frac{\theta_q - \varphi}{2}\right) \sin\left(\frac{\varphi - \theta_r}{2}\right), \end{aligned}$$

where the last line derives from the formula: $\sin a + \sin b + \sin c = 4 \sin \frac{a}{2} \sin \frac{b}{2} \sin \frac{c}{2}$ when $a + b + c = \pi$. So that we get:

$$\begin{aligned} &\mathbb{E} [\text{deg}(p, \text{Del})] \\ &= \frac{1}{2} \int_{\mathbb{R}} \int_0^{2\pi} \int_0^{2\pi} \int_0^{2\pi} \lambda^2 e^{-\lambda \pi \rho^2} |\det(J(\rho, \varphi, \theta_q, \theta_r))| d\theta_r d\theta_q d\varphi d\rho \\ &= \int_{\mathbb{R}} 2\rho^3 \lambda^2 e^{-\lambda \pi \rho^2} d\rho \\ &\quad \times \int_0^{2\pi} \int_0^{2\pi} \int_0^{2\pi} \left| \sin\left(\frac{\pi - (\theta_q - \theta_r)}{2}\right) \sin\left(\frac{\theta_q - \varphi}{2}\right) \sin\left(\frac{\varphi - \theta_r}{2}\right) \right| d\theta_r d\theta_q d\varphi \end{aligned}$$

simplified by the translation $(\theta_q, \theta_r) \mapsto (\theta_q - \pi - \varphi, \theta_r - \pi - \varphi)$ applied in the $(2\pi, 2\pi)$ -periodic function $(\theta_q, \theta_r) \mapsto \sin\left(\frac{\pi - (\theta_q - \theta_r)}{2}\right) \sin\left(\frac{\theta_q - \varphi}{2}\right) \sin\left(\frac{\varphi - \theta_r}{2}\right)$,

$$\begin{aligned} &= \frac{1}{\pi^2} \times \int_0^{2\pi} d\varphi \times \int_0^{2\pi} \int_0^{2\pi} \left| \sin\left(\frac{\theta_q - \theta_r}{2}\right) \right| \sin \frac{\theta_q}{2} \sin \frac{\theta_r}{2} d\theta_r d\theta_q \\ &= \frac{1}{\pi^2} \times 2\pi \times 3\pi = 6. \quad \square \end{aligned}$$

Proposition 9 For a given $q \in \mathbb{R}^2$ and for $\alpha \in \mathbb{R}^+$, consider the ellipse $r_c(p, q)$ parameterized by $c = (\alpha^2 \frac{x_q}{2}, \frac{y_q}{2})$.

The geometric center of $r_c(p, q)$ is the midpoint of $[pq]$, and its area is $\frac{\pi}{4} \left(\alpha x_q^2 + \frac{y_q^2}{\alpha} \right)$.

Proof. of Proposition 9 We note $E_c(x, y) := \alpha^2 x^2 - 2xx_c + y^2 - 2yy_c$ with $\alpha^2 = \frac{2x_q x_c - y_q^2 + 2y_q y_c}{x_q^2}$. If $y_c = \frac{y_q}{2}$, then $\alpha^2 x_q^2 - 2x_q x_c = 0$, and so $x_c = \alpha^2 \frac{x_q}{2}$.

$$\begin{aligned} E_c(x, y) &= \alpha^2 x^2 - 2xx_c + y^2 - 2yy_c \\ &= \alpha^2 (x^2 - xx_q) + y^2 - yy_q \\ &= \alpha^2 \left(x - \frac{x_q}{2} \right)^2 + \left(y - \frac{y_q}{2} \right)^2 - \alpha^2 \frac{x_q^2}{4} - \frac{y_q^2}{4}. \end{aligned}$$

Dividing by $\frac{\alpha^2 x_q^2 + y_q^2}{4}$, another equation of $r_c(p, q)$ is:

$$\frac{4\alpha^2}{\alpha^2 x_q^2 + y_q^2} \left(x - \frac{x_q}{2} \right)^2 + \frac{4}{\alpha^2 x_q^2 + y_q^2} \left(y - \frac{y_q}{2} \right)^2 - 1 < 0.$$

We identify, with that expression, that $r_c(p, q)$ is the translation by the vector $\frac{1}{2} \vec{pq}$ of the ellipse defined by:

$$\frac{4\alpha^2}{\alpha^2 x_q^2 + y_q^2} x^2 + \frac{4}{\alpha^2 x_q^2 + y_q^2} y^2 - 1 = 0,$$

whose center is p , and area is $\frac{\pi}{4} \left(\alpha x_q^2 + \frac{y_q^2}{\alpha} \right)$. \square

Lemma 16 Let $t > 0$, $\beta \in (0, 1)$ and

$$I_\beta(t) = \int_{\mathbb{R}} \int_{\mathbb{R}} e^{-t\sqrt{(x^2+y^2)(\beta^2 x^2+y^2)}} dy dx,$$

$$I_\beta(t) = \frac{1}{t} I_\beta(1) \leq \frac{\pi}{t} \left(1 + \ln\left(\frac{1}{\beta}\right) \right).$$

Proof. of Lemma 16

We apply, in the integral, the variables substitution: $(x, y) = (\frac{1}{\sqrt{t}}X, \frac{1}{\sqrt{t}}Y)$ with Jacobian determinant $\frac{1}{t}$.

$$\begin{aligned} I_\beta(t) &= \int_{\mathbb{R}} \int_{\mathbb{R}} e^{-t\sqrt{(x^2+y^2)(\beta^2 x^2+y^2)}} dy dx \\ &= \int_{\mathbb{R}} \int_{\mathbb{R}} \frac{1}{t} e^{-\sqrt{(X^2+Y^2)(\beta^2 X^2+Y^2)}} dY dX \\ &= \frac{1}{t} I_\beta(1). \end{aligned}$$

Then we compute an upper bound:

$$\begin{aligned} I_\beta(1) &= \int_{\mathbb{R}} \int_{\mathbb{R}} e^{-\sqrt{(x^2+y^2)(\beta^2 x^2+y^2)}} dy dx \\ &= 4 \int_0^\infty \int_0^\infty e^{-\sqrt{(x^2+y^2)(\beta^2 x^2+y^2)}} dy dx \\ &= 4 \int_0^{\frac{\pi}{2}} \int_0^\infty r e^{-r^2 \sqrt{\beta^2 \cos^2 \theta + \sin^2 \theta}} dr d\theta \\ &= 2 \int_0^{\frac{\pi}{2}} (\beta^2 \cos^2 \theta + \sin^2 \theta)^{-\frac{1}{2}} d\theta. \end{aligned}$$

On $[0, \frac{\pi}{2}]$, $(\beta^2 \cos^2 \theta + \sin^2 \theta)^{-\frac{1}{2}}$ is smaller than both $\frac{1}{\beta}$ and $\frac{\pi}{2\theta}$; on the one hand, because $(\beta^2 \cos^2 \theta + \sin^2 \theta)^{-\frac{1}{2}}$ decreases from $\frac{1}{\beta}$ to 1, on the other hand, because $(\beta^2 \cos^2 \theta + \sin^2 \theta)^{\frac{1}{2}} \geq \sin \theta \geq \frac{2}{\pi} \theta$, so that:

$$\begin{aligned} I_\beta(1) &\leq 2 \int_0^{\frac{\pi}{2}} \min\left(\frac{1}{\beta}, \frac{\pi}{2\theta}\right) d\theta \\ &= 2 \left(\int_0^{\beta \frac{\pi}{2}} \frac{1}{\beta} d\theta + \int_{\beta \frac{\pi}{2}}^{\frac{\pi}{2}} \frac{\pi}{2\theta} d\theta \right) \\ &= \pi (1 - \ln(\beta)). \quad \square \end{aligned}$$